PROCEEDINGS OF SCIENCE

Jet Production in Heavy Ion Collisions with the ATLAS Experiment

Helena Santos, on behalf of the ATLAS Collaboration*

Laboratório de Instrumentação e Física Experimental de Partículas, LIP
Av. Prof. Gama Pinto 2, Lisbon, Portugal

E-mail: helena@lip.pt

Jets are an important tool to study the hot, dense matter produced in Pb+Pb collisions at the LHC. They are produced at the early stages of the collisions and are expected to be modified as they propagate through the hot and dense medium. This leads to energy loss as well as modification of the jet structure. These proceedings highlight some of the latest jet measurements from ATLAS measured in 260 pb^{-1} and 1.7 nb^{-1} of pp and Pb+Pb collision data, respectively, at 5.02 TeV per nucleon pair. The results shown include measurements of the dijet asymmetry as a function of the leading jet transverse momentum, the suppression pattern of the internal structure, revealed when reconstructing jets with the anti-k_t algorithm using large radius parameters, and measurements of particles recoiling against the Z boson. The data provide important information to understand the strength and mechanism of jet quenching.

40th International Conference on High Energy physics - ICHEP2020
July 28 - August 6, 2020
Prague, Czech Republic (virtual meeting)

*Speaker

PoS(ICHEP2020)564

1. Introduction

Heavy ion collisions at ultra-relativistic energies take place at the Large Hadron Collider with the aim of studying the properties of the quark-gluon plasma - QGP [1]. The large acceptance and high granularity of the ATLAS detector [3] is well suited to study this state of matter and, in particular, measured jets constitute a golden probe of the QGP. The hard scattered quarks and gluons emerging from collisions evolve as parton showers that propagate through the QGP. Constituents of these parton showers are expected to emit medium-induced gluon radiation and, as a consequence, the resulting jet loses energy, a phenomenon commonly termed as *jet quenching* [2]. Accordingly, jets produced in heavy ion collisions are shown to be suppressed at a given p_{T}, relatively to a sample produced in pp collisions. Their internal structure is also shown to be modified. Results shown in this conference used data produced in 260 pb^{-1} and 1.7 nb^{-1} of pp and Pb+Pb collisions at the center of mass energy of 5.02 TeV. The Glauber Monte Carlo model [4] is used to obtain a correspondence between the total transverse energy deposited in the forward calorimeters (FCal, $3.2 \leq |\eta| < 4.9$) and the sampling fraction of the total inelastic Pb+Pb cross-section, allowing the setting of the centrality percentiles. The nuclear thickness function, $\langle T_{\mathrm{AA}} \rangle$, that accounts for the increased hard-scattering rate due to the geometric overlap between the two nuclei, is also estimated using the Glauber model [5]. Jets are reconstructed using calorimeter "towers" as input signals to the anti-k_t algorithm, with jet radius parameter sizes $R = 0.2, 0.4, 1.0$. The underlying event is estimated and subtracted event-by-event in each calorimeter layer and strip of pseudorapidity, after excluding regions under jet candidates and corrected for flow modulation [6].

2. Dijet momentum balance

The so-called dijet asymmetry was the first direct observation of jet quenching. The transverse momentum balance between two jets was shown to be modified by comparing to pp collisions or Monte Carlo predictions, resulting from configurations in which the two jets suffer different amounts of energy loss [7]. A deeper differential analysis in p_{T} was performed using a larger sample of 0.14 nb^{-1} Pb+Pb collisions data at $\sqrt{s_{\mathrm{NN}}}$ = 2.76 TeV, and in which measurements were corrected for detector effects [8]. The presented analysis uses 1.7 nb^{-1} data and measures the momentum balance up to p_{T}=562 GeV. Figure 1 shows the unfolded distributions of dijets as a function of x_{J}, the ratio between the transverse momenta of the two leading jets, for pp, 0–10%, and 60–80% Pb+Pb collisions. In central collisions, and for $158 < p_{\mathrm{T},1} < 178$ GeV, the fraction of symmetric dijets is smaller by almost a factor of 2 relatively to pp collisions, and the distribution is independent of x_{J} for $x_{\mathrm{J}} > 0.5$. For $398 < p_{\mathrm{T},1} < 564$ GeV the x_{J} trend approaches that for the pp collisions. Both in pp and peripheral Pb+Pb collisions the dependence on $p_{\mathrm{T},1}$ is much less significant. The x_{J} distributions are compared to calculations using the LIDO energy loss model [10]. This calculation uses the Pythia8 4C tune parton shower information and considers energy loss from both elastic interactions and path length dependent medium induced radiation. Momentum carried by soft partons is redistributed into the angular phase space using a simple model mimicking the hydrodynamic response. Additionally LIDO uses initial conditions from the TRENTo model to initialize a 2+1D viscous hydrodynamic simulation of the medium. The baseline calculations for pp collisions, Pythia8 4C tune with CTEQ6L1 PDFs, tend to overestimate the

contribution from balanced dijets with increasing $p_{\mathrm{T},1}$. Predictions using the LIDO transport model for two values of the QGP coupling parameter, μ, for 0–10% and 60–80% Pb+Pb collisions are also shown. They agree reasonably well with the measurement in both centrality and $p_{\mathrm{T},1}$ intervals; however they overestimate the fraction of symmetric dijets in central collisions for $p_{\mathrm{T},1} > 398$ GeV. The difference between calculations for two values of the in-medium coupling parameter μ ($\mu = 2\pi$T and $\mu = 1.5\pi$T) is typically smaller than the uncertainties on the measured x_{J} distributions and it is therefore not possible to discriminate between them [9, 10].

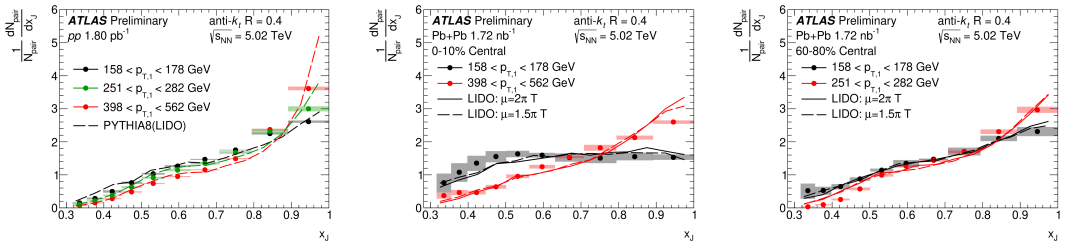

Figure 1: The x_{J} distributions for pp (left), 0–10% (middle), and 60–80% (right) centrality selections in Pb+Pb collisions. Each panel presents different leading jet $p_{\mathrm{T},1}$ ranges. The error bars show the statistical uncertainties and the boxes show the systematic uncertainties. The measured data are compared to calculations of the LIDO transport model. The left panel shows the comparison of their pp baseline to the measurement in pp collisions, whereas the center (right) panel shows the comparison of the LIDO calculations in 0–10% (60–80%) Pb+Pb collisions for two variations of the QGP coupling parameter μ. ([9, 10]).

3. Suppression of large-radius jets and its dependence on substructure

Measurements of jet fragmentation functions demonstrated that low-p_{T} particles are redistributed beyond the typical jet size of $R = 0.4$ in central collisions. For high-p_{T} particles, in contrast, the angular distributions were found to be narrower in Pb+Pb collisions than in pp interactions [11]. This observation suggests a dependence of the modification of production of jets based on their internal structure and modification of production of neighboring jets [12]. To address these expectations ATLAS has measured jets in Pb+Pb collisions using a large radius, $R = 1.0$. These jets are reconstructed with the anti-k_t algorithm by re-clustering anti-k_t $R = 0.2$ jets with $p_{\mathrm{T}} > 35$ GeV. After applying a trimming procedure, the large-radius jet constituents are re-clustered using the k_{t} algorithm in order to obtain the splitting parameter, $\sqrt{d_{12}}$, which characterizes the transverse momentum scale for the hardest splitting in the jet. The left panel of Figure 2 shows the nuclear modification factor R_{AA}, defined as the ratio of normalized yields in Pb+Pb and pp interactions, as a function of p_{T} for $R = 0.4$ and $R = 1.0$ anti-k_t jets. The former was evaluated for jets with $|y| < 2.8$ [6], while in this analysis jets are within $|y| < 2.0$. Despite this slight difference in the phase space, the results indicate a higher suppression of $R = 1.0$ re-clustered jets. It is important to notice that theoretical calculations predicting a smaller suppression when expanding the jet radius by recovering lost energy have been experimentally confirmed [13, 14]. This is not the case for the re-clustered jets where the energy radiated between $R = 0.2$ sub-jets is removed and lost energy is not recovered. The R_{AA} as a function of $\sqrt{d_{12}}$, in five centrality intervals and for $200 < p_{\mathrm{T}} < 251$ GeV, is shown in the right panel of Figure 2. The suppression for large-radius jets with a

single sub-jet ("SSJ") is different compared to the one for large-radius jets with more complex substructure. The R_{AA} decreases significantly for small values of the splitting scale followed by flattening for larger $\sqrt{d_{12}}$. This behaviour is shown to be independent on jet p_{T} up to 500 GeV [15].

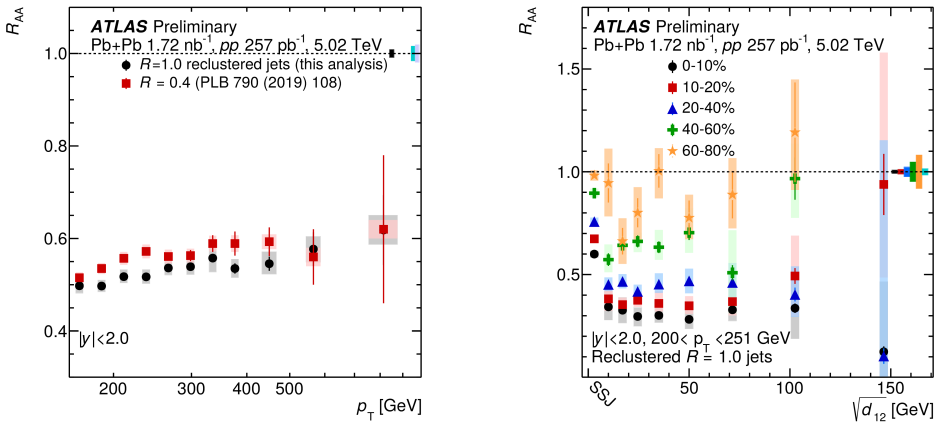

Figure 2: Left: Comparison of R_{AA} for $R = 1.0$ jets as a function of jet p_{T} to the same quantity measured with $R = 0.4$ anti-k_t jets in 0–10% centrality interval. Right: R_{AA} of $R = 1.0$ jet yields as function of the k_{t} splitting scale, $\sqrt{d_{12}}$, in five centrality intervals, and for 200 $< p_{\mathrm{T}} <$ 251 GeV. The first interval is populated only by large-radius jets with a single sub-jet. The vertical bars on the data points indicate statistical uncertainties, while the shaded boxes indicate systematic uncertainties. The systematic uncertainties on yields also include the uncertainty due to the luminosity and $\langle T_{\mathrm{AA}} \rangle$, which is correlated for all the data points. The colored boxes at $R_{\mathrm{AA}} = 1$ represent the fractional uncertainty on $\langle T_{\mathrm{AA}} \rangle$ and pp luminosity (cyan), which both affect the overall normalisation. ([6, 15]).

4. Modification of Z-tagged charged particle yields

The interest of studying jets recoiling against the Z boson lies in the fact that the electroweak boson, not being affected by the QCD matter, is therefore an excellent tag for jet energy, direction and flavour. However, the study of charged particles has the additional advantage of using events not constrained by the requirement of a reconstructed a jet, which may result in a bias towards a sample with less energy loss than average. The approach is counting the average number of charged particles per-Z, $(1/N_{\mathrm{Z}})(d^2N_{\mathrm{ch}}/dp_{\mathrm{T}}^{\mathrm{ch}}\, d\Delta\phi)$, with $p_{\mathrm{T}}^{\mathrm{ch}} > 1$ GeV and correlated with the Z boson within an azimuthal opening angle $\Delta\phi > 3\pi/4$. To quantify the modifications resulting from partons' propagation through the QGP, the ratio I_{AA} of the (per-Z) charged hadron yield in Pb+Pb collisions to those in pp collisions is used. Figure 3 shows the ratio I_{AA} as a function of the charged-hadron $p_{\mathrm{T}}^{\mathrm{ch}}$ and the hadron-to-boson p_{T} ratio, x_{hZ}, plotted for peripheral, mid–central and central collisions and for three ranges of $p_{\mathrm{T}}^{\mathrm{Z}}$. The increasing suppression with increasing centrality is visible for high $p_{\mathrm{T}}^{\mathrm{ch}}$ and x_{hZ} values, while an enhancement at low values is observed. One possible interpretation of these results is that partons produced with the Z have initially higher $p_{\mathrm{T}}^{\mathrm{ch}}$ values, but lose energy by interacting with the QGP medium, and therefore are re-distributed to lower values of $p_{\mathrm{T}}^{\mathrm{ch}}$ (or x_{hZ}). The mechanism of this energy loss is addressed by several models: the Hybrid jet quenching model [16]; a model of jet charge modification in QCD matter ($\mathrm{SCET_G}$)

[17]; the prediction generated by JEWEL ("jet evolution with energy loss") [18, 19]. This model uses perturbative QCD to describe scattering of hard partons in a hot dense medium, coupled to a parton shower; the linear Boltzmann transport and hydrodynamics model ("CoLBT-hydro"), which simulates parton transport in a hydrodynamically evolving medium, including jet-induced medium excitations [20, 21]. The results agree with the predictions, as shown in Figure 4, although Run 3 data will be valuable to better constrain the models. ([22]).

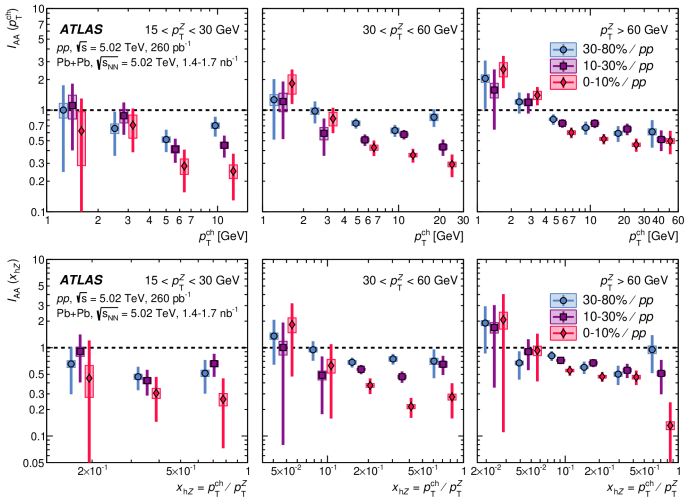

Figure 3: Ratio I_{AA} of the per-Z charged hadron yield in Pb+Pb collisions to those in pp collisions as a function of charged-hadron $p_{\mathrm{T}}^{\mathrm{ch}}$ (top panels) and the hadron-to-boson p_{T} ratio x_{hZ} (bottom panels), for $15 < p_{\mathrm{T}}^{\mathrm{Z}} < 30$ GeV (left column), $30 < p_{\mathrm{T}}^{\mathrm{Z}} < 60$ GeV (center panels) and $p_{\mathrm{T}}^{\mathrm{Z}} > 60$ GeV (right panels). Each panel shows the I_{AA} in the three categories of Pb+Pb collisions. The vertical bars and boxes correspond to the statistical and total systematic uncertainties of the data. The 30–80% and 0–10% selections are displaced horizontally for visibility, with the 10–30 % selection shown at the geometric bin center. ([22]).

References

[1] L. Van Hove, CERN-TH-4204-85. DOI: 10.1016/0375-9474(86)90623-8

[2] J.-P. Blaizot, Y. Mehtar-Tani, *J. Mod. Phys.* **24**, 1530012 (2015). arXiv: 1503.05958 [hep-ph].

[3] ATLAS Collaboration, *JINST* **3**, S08003 (2008).

[4] M.L. Miller, K. Reygers, S.J. Sanders, P. Steinberg, *Ann. Rev. Nucl. Part. Sci.* **57** 205 (2007).

[5] ATLAS Collaboration, *Phys. Lett. B* **707** 330 (2012). arXiv:1108.6018 [hep-ex].

[6] ATLAS Collaboration, *Phys. Lett. B* **790** 108 (2019). arXiv:1805.05635 [nucl-ex].

[7] ATLAS Collaboration, *Phys.Rev.Lett.* **105** 252303 (2010). arXiv:1011.6182 [hep-ex].

[8] ATLAS Collaboration, *Phys. Lett. B* **774** 379 (2017). arXiv:1706.09363 [hep-ex].

[9] ATLAS Collaboration, ATLAS-CONF-2020-017, http://cdsweb.cern.ch/record/2720247/files/ATLAS-CONF-2020-017.pdf.

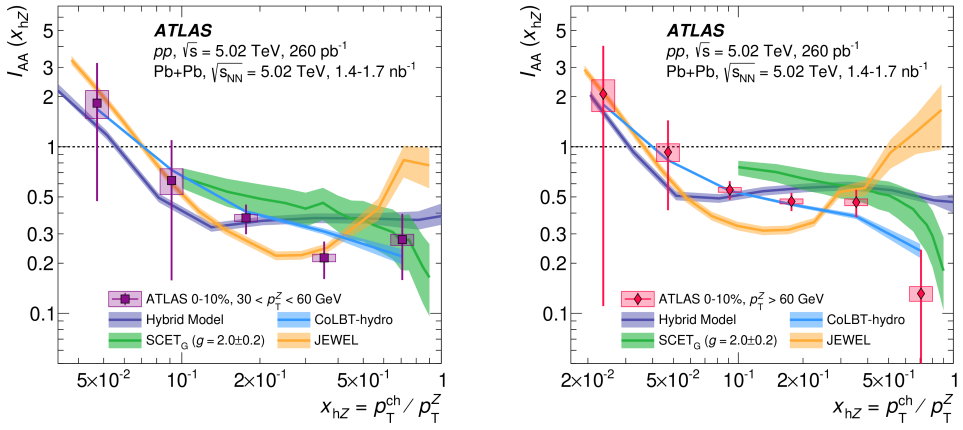

Figure 4: Ratio I_{AA} of the per-Z charged hadron yield in 0–10% Pb+Pb events to those in pp events, for $30 < p_{\mathrm{T}}^{Z} < 60$ GeV (left) and $p_{\mathrm{T}}^{Z} > 60$ GeV (right). The data are compared with calculations in the Hybrid strong/weak coupling model (dark blue curves), JEWEL (orange curves), $\mathrm{SCET_G}$ (green curves), and CoLBT-hydro (light blue curves). The vertical bars and boxes around the data correspond to the statistical and total systematic uncertainties. The shaded bands around the theoretical predictions represent the uncertainty associated with the theoretical predictions (statistical for JEWEL, Hybrid, and CoLBT-hydro, parametric for $\mathrm{SCET_G}$). ([16–22]).

[10] W. Ke, Y. Xu and S. A. Bass, *Phys. Rev. C* **100** 064911 (2019) (and references therein). url: https://link.aps.org/doi/10.1103/PhysRevC.100.064911

[11] ATLAS Collaboration, *Phys. Rev. C* **100** 064901 (2019). arXiv:1908.05264 [hep-ex].

[12] ATLAS Collaboration, *Phys. Lett. B* **751** 751 (2015). arXiv: 1506.08656 [hep-ex].

[13] I. Vitev, S. Wicks, B.-W. Zhang, *JHEP* **0811** 093 (2008). arXiv:0810.2807 [hep-ph].

[14] ATLAS collaboration, *Phys. Lett. B* **719** 220 (2013). arXiv: 1208.1967 [hep-ex].

[15] ATLAS Collaboration, ATLAS-CONF-2019-056, http://cdsweb.cern.ch/record/2701506/files/ATLAS-CONF-2019-056.pdf

[16] J. Casalderrey-Solana, D. C. Gulhan, J. G. Milhano, D. Pablos and K. Rajagopal, *JHEP* **03** 053 (2016). arXiv: 1508.00815 [hep-ph]

[17] Y.-T. Chien, A. Emerman, Z.-B. Kang, G. Ovanesyan and I. Vitev, *Phys. Rev. D* **93** 074030 (2016). arXiv: 1509.02936 [hep-ph]).

[18] R. K. Elayavalli and K. C. Zapp, *Eur. Phys. J. C* **76** 695 (2016). arXiv: 1608.03099 [hep-ph].

[19] K. C. Zapp, F. Krauss and U. A. Wiedemann, *JHEP* **03** 080 (2013). arXiv:1212.1599 [hep-ph].

[20] W. Chen, S. Cao, T. Luo, L.-G. Pang and X.-N. Wang, *Phys. Lett. B* **777** 86 (2018). arXiv: 1704.03648 [nucl-th].

[21] W. Chen, S. Cao, T. Luo, L.-G. Pang and X.-N. Wang, arXiv: 2005.09678 [hep-ph].

[22] ATLAS Collaboration, arXiv:2008.09811 [nucl-ex].